

Subsurface-Channeling-Like Energy Loss Structure of the Skipping Motion on an Ionic Crystal

J. Villette, A. G. Borisov, H. Khemliche, A. Momeni, and P. Roncin*

*Laboratoire des Collisions Atomiques et Moléculaires (CNRS UMR 8625), Université Paris Sud,
Batiment 351, F-91405, Orsay Cedex France*

(Received 18 April 2000)

The skipping motion of Ne^+ ions in grazing scattering from the $\text{LiF}(001)$ surface is studied for velocity below 0.1 a.u. with a time-of-flight technique. It is demonstrated that suppression of electronic excitation and dominance of optical phonon excitation in the projectile stopping results in an odd 1, 3, 5, ... progression of the energy loss peaks, a feature usually ascribed to subsurface channeling. The experimental findings are well reproduced by parameter-free model calculations where thermal vibrations are the dominant cause for the ion trapping and detrapping.

PACS numbers: 34.50.Bw, 34.50.Dy, 63.20.-e, 79.20.Rf

Recent studies of the interactions of ion beams with insulating surfaces of ionic crystals have revealed a large variety of original aspects such as extremely large (up to 100%) negative ion fractions in the scattered beam [1], resonant coherent excitation [2], high electron emission [3], potential sputtering [4], and projectile stopping by excitation of optical phonons [5]. All these processes depend in a crucial way upon the time spent by the projectile in the vicinity of the surface, i.e., on the projectile trajectory. This interaction time is governed by the projectile normal energy, for which the lowest value is limited to the eV range by the image charge acceleration [6]. In grazing conditions, the interaction time can be drastically increased for the peculiar types of the trajectories undergoing skipping motion on the surface. These trajectories result from the trapping of the ions in the direction z normal to the surface by the shallow potential well created by the short range repulsive potential of the surface atoms and the long range image charge attraction towards the surface.

Since the early work of Ohtsuki *et al.* [7], skipping motion of ions on top of metal and semiconductor surfaces has been extensively studied [8–11]. The successive “touch down” close to the surface associated with the skipping motion has been identified so far by the regular 1, 2, 3, ... times ΔE progression of the peaks in the energy loss spectrum [12–15], where ΔE is the energy loss associated with the first peak. This is quite different from subsurface channeling where the ions penetrate the top layer and have to undergo an odd number of close collisions with atomic planes to escape the surface, resulting in a 1, 3, 5, ... times ΔE odd progression of the energy loss peaks. The basic premise underlying these interpretations is that the projectile loses an energy ΔE by electronic excitations at the apexes of its trajectory where the distance to the target atomic planes is minimum; see, e.g., [16]. Recent experimental results on skipping motion obtained with 30 keV proton scattering from $\text{KCl}(001)$ [12] seem to confirm the well-established 1, 2, 3, ... ΔE progression for ionic crystals.

In this Letter we demonstrate that on an ionic crystal this conventional picture breaks down for *slow* collisions

($v < 0.1$ a.u.). This is because the electronic excitations are suppressed owing to the low projectile velocity and the wide band gap [17,18]. At the same time, all along the trajectory the long range Coulomb field of the projectile ion interacts with the crystal lattice, attracting the negative ions and repelling the positive ions, thus leading to the excitation of optical phonons. This becomes the dominant energy loss channel as demonstrated in [5]. Therefore a significant energy loss is not accumulated only at the immediate vicinity of the surface, as in the case of electronic stopping [18], but in a rather large z interval extending up to 30 a.u. above the surface.

The experimental setup has been described in detail elsewhere [19], and only a brief report is given here. Inside a UHV chamber, a pulsed ion or neutral beam interacts at a grazing angle ψ with a $\text{LiF}(001)$ single crystal. The scattered particles are collected on a position sensitive detector (PSD) 25 cm downstream. A slit perpendicular to the surface plane can be inserted between the target and the detector to allow separation of the final charge state with electrostatic deflectors. The coordinate on the PSD along the slit direction yields the exit angle θ while the arrival time referred to the chopper edges measures the energy of the particle. Electrons emitted during the interaction are analyzed in coincidence by 16 additional detectors surrounding the target. The target is not entirely inserted into the beam so that some ions reach the PSD without interacting with the surface, providing a valuable reference for both scattering angle and energy. The target is cleaned by grazing angle sputtering and kept at 300 °C during the experiment to avoid charging up.

To experimentally isolate the energy loss through excitation of optical phonons, it is best to choose projectiles that hardly neutralize. On a LiF target, two types of ions have been considered with ionization potential located either above (Na^+) or below (F^+ , Ne^+ , and He^+) the valence band. For these ions, resonant and Auger neutralization rates are reduced due to energy mismatch, so that important positive ion fraction is observed in the scattered beam. Although similar results were obtained with all these projectiles at velocities between 0.03 and

0.1 a.u., only those for collisions of 1 keV Ne^+ ions are detailed here.

For an incidence angle $\psi = 0.95^\circ$, 76% of the Ne^+ projectiles is scattered as positive ions in good agreement with [20,21]. Figure 1 shows the energy loss spectra of the scattered Ne^+ (Ne^0) particles; the first peak shows up at 29 (18) eV, and is followed by successively attenuated echo peaks every 47 ± 1 eV. The attenuation is faster for Ne^+ ions so that the neutral fraction increases regularly from peak to peak, reaching almost 50% for the fifth peak. The energy loss is exclusively interpreted in terms of excitation of optical phonons since neither Ne^+ nor Ne^0 projectiles suffer electronic stopping. Indeed, no electron is detected in coincidence with scattered Ne^+ ions, while at most one electron is detected in coincidence with Ne^0 particles, this latter being emitted most likely during Auger neutralization. This has been checked by shooting Ne^0 projectiles; Fig. 2 shows that they are elastically scattered from the surface. They do not produce electronic excitations, and the 1–2 eV energy loss is due to the momentum transfer to the surface atoms at the turning point of the trajectory [22]. This, in fact, corresponds primarily to the excitation of acoustic phonons.

The first peak in the Ne^+ spectrum corresponds to a single reflection from the surface, its intensity peaks around the specular direction $\theta = \psi = 0.95^\circ$; whereas the equivalent peak in the Ne^0 spectrum appears at a larger angle ($\theta = 1.8^\circ$), as the image charge attraction to the surface is no longer active on the outgoing part of the trajectory [5]. These exit angles can be converted into an energy normal to the surface. Assuming that neutralization occurs on average at the apex of the trajectory, the difference in normal energy yields the energy $E_i = 0.7$ eV gained by image charge acceleration on the incoming trajectory path [6]. For scattered Ne^0 , no phonon excitation occurs on the way out. The associated energy loss at $\theta = 1.8^\circ$ is close to half that of specularly scattered Ne^+ , the 4 eV mismatch being interpreted as the

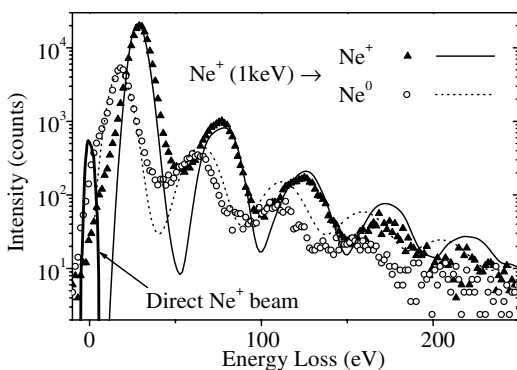


FIG. 1. Energy loss spectra for Ne^+ (\blacktriangle) and Ne^0 (\circ) particles scattered from LiF(001) after 1 keV collisions at 0.95° incidence. The results of the simulation are superimposed as lines after a 1.5 scaling factor in the energy axis.

energy defect due to Auger neutralization [5]. The interaction with phonons also explains qualitatively that Ne^+ ions scattered at more grazing angles lose more energy (Fig. 2) as they fly for a longer time close to the surface. Depending on whether neutralization takes place before or after the turning point, the Ne^0 energy loss is expected to, respectively, increase or decrease with θ . Figure 2 shows that these contributions do not compensate each other.

As the energy of the echo peaks has the same θ dependence as that of their primary peak, the energy separation is constant (Fig. 2). It is also independent of the incidence angle ψ and only changes with the projectile velocity. When ψ increases, the scattering profile of the primary peaks mirror the variation of ψ , whereas those of the echo peaks point at smaller exit angle θ , thus becoming more and more subspecular as if the associated particles had partly lost memory of the initial collision conditions. More drastic, the relative intensity F associated with the echo peaks drops exponentially with ψ . Transforming ψ into normal energy E_p (eV), we find that the fraction in the echo peaks can be well reproduced by $F = 0.17 \exp(-E_p/0.73)$ with a decay constant close to the image energy gain E_i measured above.

All the characteristics described above impose an interpretation in terms of skipping motion [10,12], although up to now and for all systems investigated the energy loss associated with skipping motion was found proportional to the number of bounces on the surface [23,24]. This is because target electronic excitation was the main mechanism for the projectile stopping. Indeed, electronic friction (stopping power) decreases exponentially with increasing projectile surface distance, reflecting the electronic density profile of the target [25]. At variance with electronic friction, projectile stopping via excitation of optical phonons

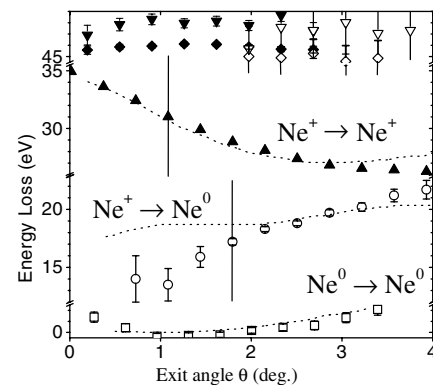


FIG. 2. Mean energy loss of the primary peaks of Ne^+ (\blacktriangle) and Ne^0 (\circ) in Fig. 1 as a function of the exit angle θ . The vertical bars indicate the FWHM of the peaks, while the error bars correspond only to the statistical uncertainty on the peak positions. On top, the peak separations from first to second and from second to third are also reported for Ne^+ (\blacktriangledown , \blacklozenge) and Ne^0 (\triangledown , \diamond). The mean energy loss associated with collisions of 1 keV Ne^0 at 1.8° is displayed (\square) at the bottom. Dotted lines are from the simulation.

remains substantial up to distances of 30 a.u. above the surface and is therefore sensitive to the larger part of the ion trajectory.

Model calculations have been carried out with three independent ingredients introduced step by step. These are the energy loss characteristics of the trapped trajectories, the trapping mechanism, and the neutralization process.

(1) The classical trajectories are calculated from the total potential resulting from the binary interaction potentials with individual lattice sites and image charge attraction to the surface. The binary interaction potentials were derived by a Hartree-Fock method. As a first approximation, both the stopping power due to excitation of optical phonons and the effective image potential deriving from the polarization of the crystal can be evaluated from the dielectric response function $[\varepsilon(\omega) - 1]/[\varepsilon(\omega) + 1]$ [26,27]. It is derived (local approximation) from the optical data for dielectric constant $\varepsilon(\omega)$ [28]. Figure 3 displays the energy loss accumulated over a trajectory as a function of the total energy E_p in the direction normal to the surface. For trapped trajectories ($E_p < 0$), the curve exhibits a maximum resulting from the balance between two opposite contributions. The deeper the ions are trapped in the potential well, the closer to the surface lies the outer turning point but also the shorter is the length of the bound trajectory. The maximum energy lost during one bounce by trapped ions is close to $2\Delta E$, i.e., twice that undergone by specularly reflected ions provided their incident normal energies are above half an electron volt. Hence an integer number of bounces on the surface directly generates the observed near $1, 3, 5, \dots \Delta E$ energy progression.

(2) Regarding the projectile trapping mechanism, several processes have been invoked: inelastic energy transfer [9], terrace edges [12,29], and thermal vibrations [10,12,16,29,30]. The width of the scattering profiles gives a hint on the importance of the thermal motion of the target ions. Because Ne^+ ions are sensitive to a charging up of the target below 200 °C, the temperature influence is best probed by Ne^0 projectiles at an incidence angle of 1.8° chosen to match the Ne^0 exit angle of Fig. 1. Figure 4 presents the scattering profiles measured

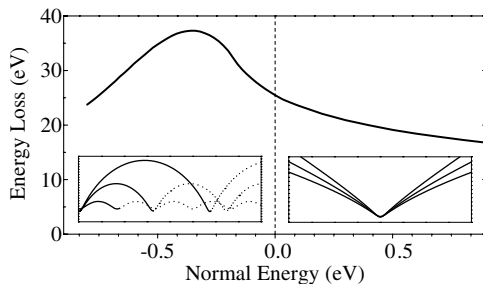


FIG. 3. Calculation of the energy loss to optical phonons on an ideally flat surface as a function of the normal energy E_p . For trapped periodic trajectories ($E_p < 0$), it is calculated along one full period. The insets display model trajectories.

at 30 and 600 °C. Note that a substantial fraction of the profiles lies below the critical angle $\theta_c = \sin^{-1} \sqrt{E_i/E_0}$ beyond which a scattered Ne^+ ion could not escape from the image attraction $E_i = 0.7$ eV, E_0 being the incident energy [31]. In other words, trapping as well as detraping results from the broadening of the angular profile at each bounce. Since target atoms do not have time to move during the collision time, a simple trajectory calculation has been developed with thermally displaced atoms [10] that readily produces the observed angular straggling (Fig. 4). Note that the latter does not require exchange of normal energy with the surface, but rather derives from the approximate local flatness probed by the ions close to the surface.

At this point, switching on the image potential and the coupling with optical phonons described in (1), the calculations directly produce the proper skipping fraction and relative peak separation (Fig. 1) as well as the pronounced energy loss dependence of Ne^+ ions with the exit angle (Fig. 2). The rapid energy broadening of the echo peaks is also reproduced; it derives from the dispersion of the trapped trajectories. Only the 7 ± 1 eV FWHM width of the first energy loss peak associated with single scattering is underestimated. The agreement is achieved by inclusion of randomly distributed terraces with up/down monatomic steps. As the ion flies over the “up/down” steps, the interaction time with the surface increases/decreases. For a reasonable mean terrace length of 1000 a.u. [12] used in the simulation, almost every ion encounters a terrace edge at an altitude z below 30 a.u., where the coupling to optical phonons is active. It is worth noting that the steps can also lead to trapping, though this aspect remains marginal.

(3) As for the neutralization process, the observed neutral fraction is reproduced by absorbing the Ne^+ flux with a neutralization rate $\Gamma = \Gamma_0 \exp(-z/z_n)$ a.u., with $z_n = 1.5$ a.u. taken from Ref. [20] and $\Gamma_0 = 0.0008$ a.u. the adjusted constant. This readily produces a reasonable attenuation of the successive echo peaks in the Ne^+ spectrum indicating that the surface reflectivity is rather high in spite of the few thousand a.u. spanned during

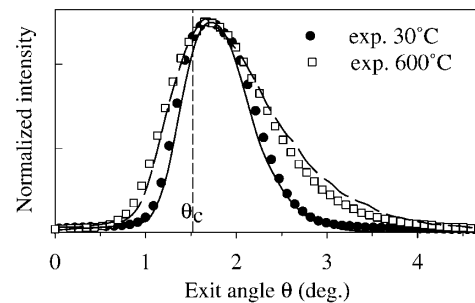


FIG. 4. Scattering profile measured with Ne^0 incident at $\psi = 1.8^\circ$ for a target at room temperature (\bullet) and at 600 °C (\square). The line plots are for the simulation, while the vertical line is set at the critical angle θ_c below which Ne^+ ions would become trapped (see text).

each skip. To keep the computation time reasonable, the spectrum associated with scattered Ne^0 is approximated assuming that once formed all along the Ne^+ trajectory, the Ne^0 particles interact with a perfect surface. This is enough for a fair description of the Ne^0 energy loss spectrum (Fig. 1), but the lack of angular straggling for particles neutralized before the impact prevents a reliable description of the θ angular dependence of the Ne^0 energy loss (Fig. 2). Another remarkable prediction is the increase of the neutral fraction with the energy loss. This outlines that, as the more loosely trapped Ne^+ ions are released first, neutralization is slowly becoming the major detrapping mechanism, even if this effect is overestimated by the present neutralization parameters.

Although the spectral features are well reproduced, the calculation underestimates the energy loss by almost 30%, and the results of Figs. 1 and 2 have been scaled accordingly. We attribute this discrepancy to the approximate character of the local response theory for the short projectile surface separation, where the field of the projectile varies significantly on the scale of the surface unit cell as already mentioned in [5]. Since complete information on the dielectric constant $\epsilon(k, \omega)$ (k wave vector) is not available at present, a quantitative agreement cannot be reached. Nevertheless, we believe that the qualitative agreement of a parameter-free calculation with the multiple aspects of the experimental data is sufficient for the present purpose.

To summarize the model analysis, the thermal motion of target ions efficiently guides some ions to exit angles below the critical angle θ_c where they become trapped, the same angular straggling (or Auger neutralization in case of neutral outgoing particles) being responsible for a possible projectile detrapping at each bounce. Along the trapped trajectories, the interaction with optical phonons in each skip gives rise to approximately twice as much energy loss as in regular specular reflection resulting in a 1, 3, 5, ... ΔE progression of the peak location in the energy loss spectrum of Ne^+ ions. For 500 eV Ne^+ projectiles, the energy lost in each skip amounts to 42 eV, almost 10% of the incident energy suggesting that the skipping motion could be an efficient way to softly slow down the projectile ions. Similar skipping motion is observed for various positive ions and for F^- ions formed on the surface.

In conclusion, we have presented a detailed study of the skipping motion of keV Ne^+ projectiles interacting at grazing angles with a LiF(001) surface. Because of the suppression of electronic excitations by the wide band gap, the projectile stopping via excitation of optical phonons becomes the dominating energy loss channel. In this context we find that the conventional assignment of the separation between the energy loss peaks to specific trajectories breaks down. The skipping motion of ions results in a 1, 3, 5, ... ΔE progression of the energy loss peaks usually considered as a signature of subsurface channeling. Our results are well reproduced by the model calculations.

The authors are indebted to M. Barat and J. P. Gauyacq for fruitful discussions and careful reading of the manuscript.

*Corresponding author.

Electronic address: ronc@lcam.u-psud.fr

- [1] A. G. Borisov, V. Sidis, and H. Winter, Phys. Rev. Lett. **77**, 1893 (1996).
- [2] C. Auth *et al.*, Phys. Rev. Lett. **79**, 4477 (1997).
- [3] M. Vana *et al.*, Europhys. Lett. **29**, 55 (1995).
- [4] T. Neidhart *et al.*, Phys. Rev. Lett. **74**, 5280 (1995).
- [5] A. G. Borisov *et al.*, Phys. Rev. Lett. **83**, 5378 (1999).
- [6] C. Auth *et al.*, Phys. Rev. Lett. **74**, 5244 (1995).
- [7] Y. H. Ohtsuki, K. Koyama, and Y. Yamamura, Phys. Rev. B **20**, 5044 (1979).
- [8] K. Kimura, M. Hasegawa, and M. Mannami, Phys. Rev. B **36**, 7 (1987).
- [9] K. J. Snowdon, D. J. O'Connor, and R. J. MacDonald, Phys. Rev. Lett. **61**, 1760 (1988); B. W. Dodson, Phys. Rev. Lett. **62**, 2421 (1989); K. J. Snowdon, Phys. Rev. Lett. **62**, 2422 (1989).
- [10] R. Pfanzelter *et al.*, Nucl. Instrum. Methods Phys. Res., Sect. B **83**, 469 (1993).
- [11] R. Pfanzelter *et al.*, Phys. Rev. B **57**, 15496 (1998).
- [12] K. Narumi *et al.*, Surf. Sci. **303**, 187 (1994).
- [13] F. Stölzle and R. Pfanzelter, Surf. Sci. **251**, 883 (1991).
- [14] J. H. Rechten, W. Mix, and K. J. Snowdon, Surf. Sci. **248**, 27 (1991).
- [15] H. Winter and M. Sommer, Phys. Lett. A **168**, 409 (1992).
- [16] M. Kato, T. Iitaka, and Y. H. Ohtsuki, Nucl. Instrum. Methods Phys. Res., Sect. B **33**, 432 (1988).
- [17] C. Auth *et al.*, Phys. Rev. Lett. **81**, 4831 (1998).
- [18] P. Roncin *et al.*, Phys. Rev. Lett. **83**, 864 (1999).
- [19] V. A. Morosov *et al.*, Rev. Sci. Instrum. **67**, 2163 (1996).
- [20] T. Hecht *et al.*, Phys. Lett. A **220**, 102 (1996).
- [21] F. W. Meyer *et al.*, Nucl. Instrum. Methods Phys. Res., Sect. B **125**, 138 (1997).
- [22] While writing this manuscript we became aware of the work by A. Mertens and H. Winter, Phys. Rev. Lett. (to be published).
- [23] H. Winter, J. Phys. Condens. Matter **8**, 10149 (1996).
- [24] H. Sakai, R. Yamashita, and Y. O. Ohtsuki, Nucl. Instrum. Methods Phys. Res., Sect. B **96**, 494 (1995).
- [25] J. I. Juaristi *et al.*, Phys. Rev. Lett. **84**, 2124 (2000).
- [26] P. M. Echenique and A. Honie, Ultramicroscopy **16**, 269 (1985).
- [27] F. J. Garcia de Abajo and P. M. Echenique, Phys. Rev. B **46**, 2663 (1992).
- [28] Palik and Hunter Handbook of Optical Constants in Solids (Academic Press, New York, 1985).
- [29] D. J. O'Connor and K. J. Snowdon, Nucl. Instrum. Methods Phys. Res., Sect. B **58**, 360 (1991).
- [30] R. Smith, D. J. O'Connor, and E. I. von Nagy Felsobuki, Vacuum **44**, 311 (1993).
- [31] T. Miyamoto, T. Iitaka, and Y. H. Ohtsuki, Nucl. Instrum. Methods Phys. Res., Sect. B **48**, 330 (1990).